Report for 2004GA56B: Seismic imaging of fracture systems in crystalline rock

There are no reported publications resulting from this project.

Report Follows

Final Report
Project G-35-B99
Covering period: March 2004 through February 2005

Seismic imaging of fracture systems in crystalline rock.

Sponsored by:
Georgia Water Research Institute

Principal investigator: Dr. Leland Timothy Long,
Professor of Geophysics
Georgia Institute of Technology
School of Earth and Atmospheric Sciences
Atlanta, GA 30332-0340
(404) 894-2860 (Office) (404) 894-5638 (FAX)

Graduate Assistant: Tatiana Toteva
Georgia Institute of Technology
School of Earth and Atmospheric Sciences

Seismic imaging of fracture systems in crystalline rock

Executive Summary

A critical need in understanding open or fluid filled fractures in crystalline rock is the ability to reliably identify fractures and to characterize their source zones. This research is directed toward testing two advanced seismic imaging techniques that have not been used previously in hydrology. One technique is scattering inversion, which is a three-dimensional extension of CDP (common depth point) stacking and tomography. The other technique is surface wave inversion to monitor changes in the water content in shallow soils. Together, these two techniques could image the fracture systems and surface source zones characteristic of the Piedmont province. The tests were performed in the Panola Mountain Research Watershed, a watershed typical of the Piedmont Province.

For the shallow source aquifers above the crystalline rock we compared seismic traces over time to identify changes in seismic response related to changes in water content. In the Rhodes-Jordan Well Field (RHWF) near Lawrenceville, GA we observed significant changes in the seismic signature when comparing data obtained during pumping and without pumping of water out of the fractures. However, the cause and location of the perturbation could not be uniquely defined.

At the Panola Mountain Research Watershed (PMRW) we tested the capability of trace differences (using identical sources, recording sites and instruments) to monitor soil moisture content. The surface wave data from a line parallel to the streambed in the valley floor showed significant variations in character with time. The analysis can thus be used as a water content monitor if calibrated against water level data.

At the PMRW we also established an array of sensors on the exposed rock. In the area of exposed rock, we have preliminary results from a modified formulation of the scattering inversion. The data suggest that we will be able to identify and map fractures and surface features.

These two techniques when applied to appropriate areas could be important tools for the evaluation of water resources in crystalline rocks. We have demonstrated that they have the potential of providing quantitative data on the fractures and the near-surface water sources.

The research results have contributed in whole or in part to 6 talks at national and regional meetings. Two paper describing the techniques are in preparation. The next step in developing these as viable exploration and monitoring techniques is to refine the techniques with further tests, more carefully define the types of areas where they can be applied and establish a protocol for their application.

Seismic imaging of fracture systems in crystalline rock

Statement of critical regional water problem

In areas like the Georgia Piedmont, that are underlain by fractured and unweathered crystalline rock, water resources are limited to surface reservoirs and shallow wells. Because surface reservoirs are approaching full development, and because new large surface reservoirs are difficult to site, the water needs of the expanding suburban and urban areas in central Georgia will have to come from alternate sources. These sources include conservation and ground water. In crystalline areas the near-surface ground water supplies, usually exploited by shallow wells, have a capacity that is limited by thin soils, but there exist fracture systems in the crystalline rocks that can supply significant amounts of water because they draw from a wide area and from many near-surface shallow aquifers. These fractures and their supply system offer a mechanism for efficient pumping of water for municipal water supplies. Fracture systems with production potential are difficult to locate and evaluate, and, hence, are underutilized. A growing need exists for methods to detect and characterize open productive fracture zones in the metamorphic and igneous rocks of the Georgia Piedmont. Some communities, for example Lawrenceville, have successfully tapped such fracture zones as a supplement to surface reservoirs. An increasing number of Counties and local governments are evaluating ground water in fractures as a primary or supplemental source to their existing surface water systems because in periods of drought, surface reservoirs and shallow wells will be depleted before deep fractures. A more important aspect of productive fracture zones is to understand the geometry of the productive fractures and their relation to near-surface water sources. A quick and non-intrusive method to locate and evaluate fracture zones that are productive could save on drilling exploration techniques and expand available water resources.

Nature, scope, and objectives of the research.

In this work we tested the ability of new seismic analysis methods to image and evaluate fractured rock aquifer systems. The fractured rock aquifer system studied in this research consisted of a fracture zone in crystalline rock and the shallow storage or collection zones at the surface. This is a system that would be typical for well fields in crystalline rock, such as those found at the Rhodes-Jordan Well Field in Lawrenceville, GA, or the Panola Mountain Research Watershed (PMRW). Figure 1 is a simplified cross section of the PMRW, which served as the primary test area for seismic techniques.

Our hypothesis is that new seismic analysis methods can image and quantify fractured rock aquifer systems. We hypothesize that the fractures can be imaged using high-frequency scattered or reflected waves using scattering inversion, a technique analogous to the stacking process in reflection seismic data analysis or pre-stack migration. Furthermore, we hypothesize that the near-surface source aquifer can be imaged and monitored using surface waves. Most importantly, we hypothesize that the addition or withdrawal of water from these aquifers can be monitored by observing slight changes in the waveform over time. Specifically, we proposed to evaluate coda envelope inversion in an area of known fracture zones in order to assess whether

fractures can be detected on a scale of 100 meters. And, we proposed to test the differential surface wave technique for monitoring variations in water content in a surface aquifer.

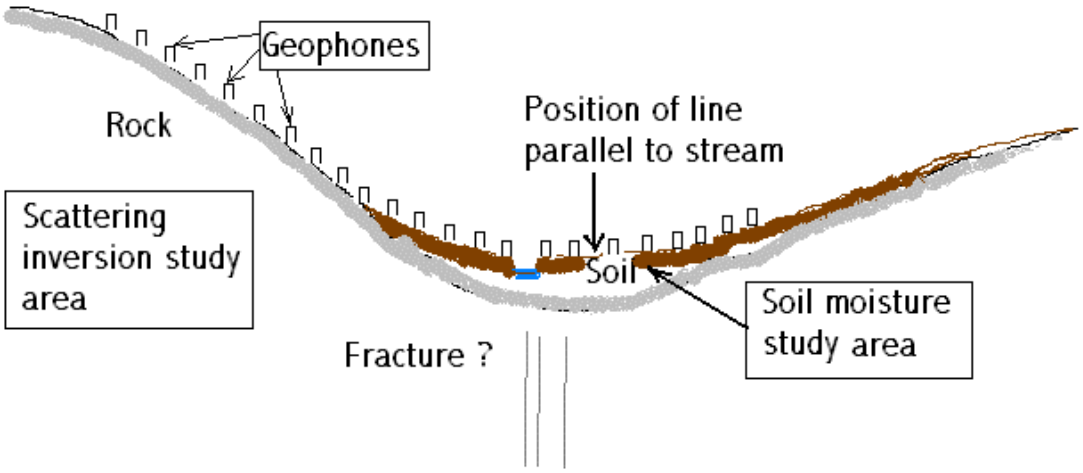

Figure 1. Cross section of the Panola Mountain Research Watershed showing proposed locations of geophones.

The PMRW is a small watershed that is a model for many similar watersheds in the Piedmont Province of Georgia. The advantage of the PMRW for this research is that it is small and has been extensively studied. The small scale is an advantage for seismic data acquisition because smaller non-destructive sources can be used. The disadvantage is the attenuation of the higher frequencies needed to resolve details. The exposed rock portion of the study area (left side of figure 1) is where the scattering inversion experiment was performed to attempt to detect a possible fault/fracture zone below the axis of the valley. The lack of soils greatly reduced the attenuation of high frequency seismic waves. The PMRW provided a clean rock surface to test the scattering inversion without interference from surface sediments. However, the location and extent of fractures in the crystalline rock is only partially documented at the PMRW. The Rhodes-Jordan Well Field in Lawrenceville was studied as a site where the fractured rock is below a layer of sediment or fill, but where the fractures have been documented by geophysical logs from numerous test wells.

At the PMRW the soil fill in the valley were used to test the ability of surface waves to monitor water content. We used surface waves to measure the velocity structure of the shallow soil layer before and after a significant rain event. By comparing the seismic velocity perturbations with stream flow and soil moisture measurements (from independent USGS data) we proposed to determine the effectiveness of surface wave perturbation measurements to monitor water content in the soil aquifer. Conventional seismic refraction and surface wave interpretation were used to determine the thickness and structure of the soil layer.

Specific objectives and summary of results:

Objective 1: The first two objectives relate to the Rhodes-Jordan Well Field (RJWF). First, we proposed to obtain at least two new sets of data in order to improve the array design for sensitivity to reflections and their perturbations under different pumping rates. In a field trip

during December 2003, we obtained data for the analysis of shallow structures. In a later field trip on October 8, 2004, we used modified field measurement techniques and a more repeatable source to attempt to obtain temporal perturbations in reflections from the known fractures.

Objective 2: We proposed to complete an analysis of the shallow structure in order to assist in the interpretation of temporal changes in scattering. The details of this analysis are given in Appendix I. The analysis used conventional stacking (averaging) techniques to enhance arrivals from the depths of the fractures identified in well logs provided by the US Geological Survey. The analysis showed that the cessation of pumping produced measurable changes in the seismic response. We were not able to determine in this case whether the change was due to changes in water pressure within the fracture or to changes in water content in the sediments. A significant limitation at the RHWF was that the surface waves dominated the record in the time window expected for arrival of many of the waves scattered off of the fractures. Hence, a coda sufficiently clean for scattering inversion could not be obtained at this site. Also, the frequency response of the geophones located in near-surface soils could not be tested for frequencies above 400 Hz, and those frequencies are needed for a reliable scattering inversion.

Objective 3: We had demonstrated a need to improve the high-frequency content and repeatability of our source. Consequently, we have designed a modified weight drop mechanism that produces the repeatable and relatively small signals needed in this work. The amplitudes of the signals generated need not be large because we are operating at comparatively short distances, typically less than 30 meters.

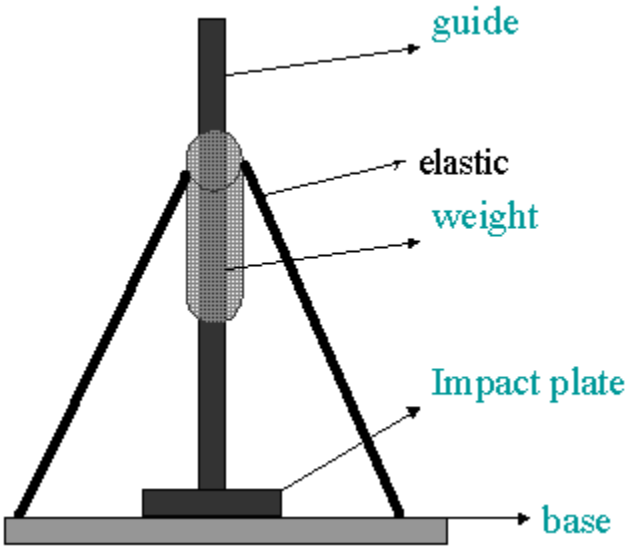

Figure 2. Simplified diagram of controlled source.

The source consists of a weight that slides down a guide. The impact plate on the bottom produces the high-frequency source function and the base, which is weighted or attached to the ground, transmits the signal into the ground. The elastic bands serve to accelerate the mass to provide a stronger strike within a short distance. The guide and impact plate design assure that

the signal for each shot is similar. The trigger is placed on the base. An additional elastic band was attached later to prevent multiple signals caused by a bouncing of the weight.

Objective 4: In the PMRW, we will lay out two repeatable seismic lines, one parallel to the valley and one perpendicular. We have set up two orthogonal lines of 16 geophones each in the valley. The first line is parallel to the stream. The second line starts at the center of the first line and extends up hill, forming a "T" configuration. The upstream end of the first line is shown in Figure 3. The area was chosen because it is populated with many water level monitoring pipes placed into the ground.

Figure 3. Picture of the first line parallel to the streambed (to the right of the figure).

Objective 5 and 6: We proposed to take sets of surface wave measurements along the lines during periods of similar rainfall and at different times to obtain data during different phases of significant rain events. We have obtained numerous sets of data on the line parallel to the streambed and the results are illustrated in Appendix II. The data in Appendix II show that changes on the order of 5 percent can be expected in the surface wave velocities when comparing records obtained before and after significant changes in water level in soils. The technique can resolve velocity changes of less than 1 percent.

Objective 7: By moving the source over many sites on the crystalline rock outcrop we proposed to provide data for a scattering inversion to identify fractures in the surrounding rock. The scattering inversion will be performed using arrays of geophones on the outcropping unweathered rock. This has the advantage of not attenuating the source and will allow excitation of more high-frequency energy. The results of this analysis are in preparation for presentation at the American Geophysical Union meeting in May 2005. The preliminary details of this analysis are given in Appendix III. A significant problem in measuring seismic vibrations on hard rock is

the coupling of the geophones to the rock. This was made more difficult by the fact that we needed to record frequencies in the range of 500 to 1000 Hz. At these frequencies, the geophones must be very tightly coupled to the rock. We tried making mounts with cement and screwing the geophones into the mounts and the traditional technique of weighting the geophones with sand bags. Neither of these worked satisfactorily. The most successful technique was to mold the geophones into the rock face with modeling clay and use the sand bags to help maintain contact.

Objective 8: We proposed to perform a comparison of the seismic interpretation with data from water monitoring sites provided by the USGS. Because of the character of these measurements, we did not consider this a significant comparison. The data available from the USGS close to the test site is obtained at the upper weir. Unfortunately, this weir does not block water flow in the valley sediments, and a significant portion of the water outflow is not registered. The fate of the water was one aspect studied, but not solved by the Georgia Tech environmental field methods course EAS4610. We also obtained refraction data from the upper weir to our test site to assist Dr. Marc Stieglitz in his investigation of the water budget of the smaller watershed. Dr. Stieglitz is making a detailed study of the USGS water flow data.

Statements of Collaboration:

The field research has been designed to supplement research performed by the U.S. Geological Survey. Personnel familiar with the Lawrenceville and Panola Mountain sites have visited our field site and suggested areas of potential additional work. The seismic techniques have proven valuable in identifying underground structures. The surface wave technique is effective in determining depth to basement and locating anomalous structures in profiles. We plan to continue development of these techniques. The preliminary results of scattering inversion on the hard rock suggest that this technique could be very effective in identifying fractures.

As part of our collaborative efforts, we have obtained a line of data extending from the upper weir to our test line. This data was designed to help Marc Stieglitz in understanding the fate of water bypassing the upper weir.

Training Activities

One Ph.D. student, Tatiana Toteva, in geophysics was partially supported by this research. The results of the scattering inversion will contribute to her Ph.D. thesis. Two undergraduate students, Chris Keiser and Michael Chen, received partial support working on this research. Chris Keiser assisted in some of the fieldwork and Michael Chen assisted in computer programming.

The Panola Mountain Research Watershed during spring semester, 2005, was made the topic for the capstone senior course, environmental field methods. The course included 14 students who obtained field data and analyzed the data as part of their studies. The topics ranged from atmospheric pollution to water temperature. One student used seismic data in a seismic reflection experiment and another student used seismic data in a refraction study. A third student interpreted ground penetrating radar data obtained as part of the course. The results of these

studies were written up in a final report and presented at a class symposium. Copies of the report have been given to the U.S. Geological Survey, water resources division, in Atlanta.

One MS thesis will be the direct result of studies in the Panola Mountain Research Watershed. Gabriel Hebert has obtained data and will be writing his M.S. thesis on a comparison of ground penetrating radar and seismic techniques. The study area brackets the trench area extensively studied by the U.S. Geological Survey and associated scientists. The thesis is directed to, first, an evaluation of the advantages of the two techniques and, second, to solving problems related to flow of water down slope. The significant question to be answered by this analysis is whether fractures can be found that contribute to diverting fluid from the soil.

Information Transfer

Final report: The contributions of this research are summarized in this final report.

Talks at professional meetings: The research results have contributed in whole or in part to 6 talks at national and regional meetings. The titles and abstracts for these talks are listed below

Toteva, Tatiana, and L.T. Long. Differential coda imaging of fractures, American Geophysical Union Meeting, San Francisco, December 2003.

Abstract: Coda waves have been extensively used to characterize the scattering and attenuation properties of the earth interior. Their sensitivity to earth's heterogeneity makes them a potential tool for mapping fractures within the earth crust and monitoring changes in their properties. Some lab experiments (Sneider, 2002) show that small change in the temperature can lead to very subtle change in the velocity, which is detectable in the coda waves and not in the direct arrivals. We used a finite difference coda to generate acoustic waves, traveling in a fractured medium. A small change in the velocity within the fractures is not visible on the seismogram. The effect of that change becomes obvious if one takes the difference in the seismograms. In the case of elastic medium such differences should be even more prominent. One possible application of this differential coda imaging technique is detection and monitoring of open productive fracture zones. These fracture zones may offer larger flow rates and capacity than shallow surface wells. Use to monitor changes in water pressure associated with initiation or stopping on pumping on production wells.

Long, L.T., and Toteva, Tatiana. Differential surface wave analysis: a technique to monitor changes in fluid flow in shallow aquifers. American Geophysical Union Spring Meeting, Montreal, Canada. May 2004

Abstract: The objective of differential surface-wave analysis is to identify temporal perturbations in the shear-wave velocity, and hence ultimately to monitor water saturation and/or water pressure in shallow soils. We directly measure perturbations in velocity by a comparison of seismic traces obtained before and after a change in the water saturation. Perturbations in phase velocity are measured as a function of frequency in the frequency domain of the difference of normalized traces. The perturbed structure can then be computed relative to a reference structure that need only approximate the actual structure.

Michael Chen, Processing the perturbation method. 76th Annual Meeting, Eastern Section Seismological Society of America, Virginia Polytechnic Institute and State University, Blacksburg, Virginia. October 31 to November 1, 2004.

Abstract: A software implementation of a perturbation method for shear-wave velocity inversion from surface waves is presented. Signals from Seismic Unix data files are extracted and processed with the multiple-filter technique. The dispersion curves are then treated as perturbations to the reference dispersion from a library of pre-computed curves. Finally, the corresponding reference velocity profile is perturbed in the equivalent way to yield the shear-wave profile. Orthogonal functions of velocity with respect to depth are used as the perturbation functions. The software's code will be freely available under an open-source license.

Tatiana Toteva, and L.T. Long, Differential Approach for Detecting Temporal Changes in Near-Surface Earth Layers, 76th Annual Meeting, Eastern Section Seismological Society of America, Virginia Polytechnic Institute and State University, Blacksburg, Virginia. October 31 to November 1, 2004.

Abstract: The physical parameters (shear wave velocity, density, porosity, etc.) of near-surface soils and weathered rocks have been extensively studied for the purposes of geotechnical engineering, hydrology, oil and gas exploration etc. The possibility of using geophysical techniques for monitoring changes within this upper layer has gained big popularity within the recent years. The objective of this study is to develop a differential technique for detecting subtly velocity changes within the soil layer. The differential technique is based on a study of the difference between two normalized traces taken at successive time intervals. The differences are interpreted as perturbations to a structure. This study has applied the differential technique to Rayleigh waves. We hypothesized that fluid penetration due to natural causes (rainfall) or pumping of fluids, would lead to changes in the shear wave velocity, which could be detected on the differential seismograms. In the traditional approach the soil layer is studied by inverting the phase velocity dispersion curve for the velocity structure. Instead of the phase velocity we use group velocity for inversion curve. Group velocity depends on phase velocity and the change of the phase velocity with frequency. Hence, we hypothesized that group velocity would be more sensitive to subtle changes in the velocity structure. The technique was tested for two different types of soil perturbations. We acquired data before and after heavy rain in the Panola Mountain Research Watershed to test the effect of variations in water table and soil moisture. At a second site, we tested a more controlled perturbation by pumping water into the soil at a depth of about 1.0 meter. Important factors in the acquisition of this data were the use of a repeatable weight-drop source and a secure and repeatable geophone placement. Our results show that the fluid penetration I the soil causes phase changes and time shifts, detectable on the differential seismograms.

Tatiana Toteva and L.T. Long, ESSSA

Tatiana Toteva, A differential Approach for detecting subtle changes in the near-surface earth layer, Graduate Student Symposium, School of Earth and Atmospheric Sciences, November, 2004.

Abstract: The near-surface earth layer includes the soil layer and the near-surface rocks. Its physical parameters (shear wave velocity, density, porosity etc.) have been extensively studied for the purposes of geotechnical engineering, hydrology, oil and gas exploration etc. The idea of developing techniques for monitoring changes within this upper layer has gained big popularity within the recent years. The objective of this study is to develop a differential technique for detecting subtle velocity changes within the soil layer. We are targeting he upper few meters. The technique utilizes Rayleigh waves. Wee hypothesized that fluid penetration due to natural causes (rainfall) or pumping of fluids, would lead to changes in the shear wave velocity, which could be detected on the differential seismograms. In the traditional approach the soil layer is studied by inverting the phase velocity dispersion curve for the velocity structure. Instead of using the phase velocity we used group velocity inversion curve. Group velocity depends on phase velocity and the change of the phase velocity with frequency. We hypothesized that group velocity would be more sensitive to subtle changes in the velocity structure. The technique was tested at two different soil sites. We acquired data before and after heavy

rain in Panola Mnt., GA and during fluid pumping at the ATL site (Atlanta, GA). We used a repeatable weight-drop source and 16 geophones (central frequency 16 Hz). Our results show that the fluid penetration in the soil causes phase changes and time shifts, detectable on the differential seismograms.

Toteva, Tatiana, and L. T. Long. A scattering inversion experiment to identify fractures on a granite outcrop. American Geophysical Union Meeting, New Orleans, May, 2005.

Abstract: A critical need in understanding open or fluid filled fractures in crystalline rock is the ability to identify these fractures, to characterize their source zones, to map flow paths within the fractures, and to assess residence time of water in the system. Fractures are an important component in the water resources of areas where crystalline rocks crop out at the surface. We have attempted to use scattered waves to identify and map fractures in a crystalline rock. Our research was conducted at the Panola Mountain Research Watershed (PMRW), GA. The scattering technique was tested in an area of exposed rock. We used 16 geophones, 100Hz each, placed in a circular array with diameter of 16m. A major effort was taken towards suppressing resonances in the geophones at high frequency. We used clay to better attach the geophones to the outcrop and sand bags to weight the instruments down to suppress the high frequency resonance. A small weight drop source was designed to generate high frequency input signal. The source provides signals in the 300 to 800 Hz range. The source was moved about the array in distance ranges of 5 to 60 meters. The recorded signals were highly filtered to pass only waves above 500 Hz. In processing the data, the distance is obtained from the travel time and direction to the scattering fracture is obtained by using apparent velocity across the array. The technique provides a theoretical way to map positions of varying scattering efficiency and hence the location of fractures.

(note: the analysis for this paper is in preparation. Background information and draft version are given as part of Appendix III)

Pubications: We plan to prepare two papers on data from this study. The first will be an analysis of the scattering inversion from data obtained on the exposed rock. The second will be the analysis of temporal changes in the velocity along the test line parallel to the streambed in the Panola Mountain Research Watershed. The first will document the technique for identifying fractures and the second will propose this as a means to document and monitor ground water. Depending of the results, the M.S. thesis by Gabriel Hebert could lead to a publication on the comparison of seismic and ground penetrating radar techniques.

Appendix I.

Analysis of reflection data from the Rhodes-Jordan Well Field

Introduction

The Rhodes-Jordan Well Field is operated by the city of Lawrenceville, Ga. It is located in Gwinnett County, Georgia (Figure 1.0). The basement rocks are metamorphosed igneous and sedimentary rocks of the Piedmont province of central Georgia. In this area they are relatively unweathered and of granitic composition.

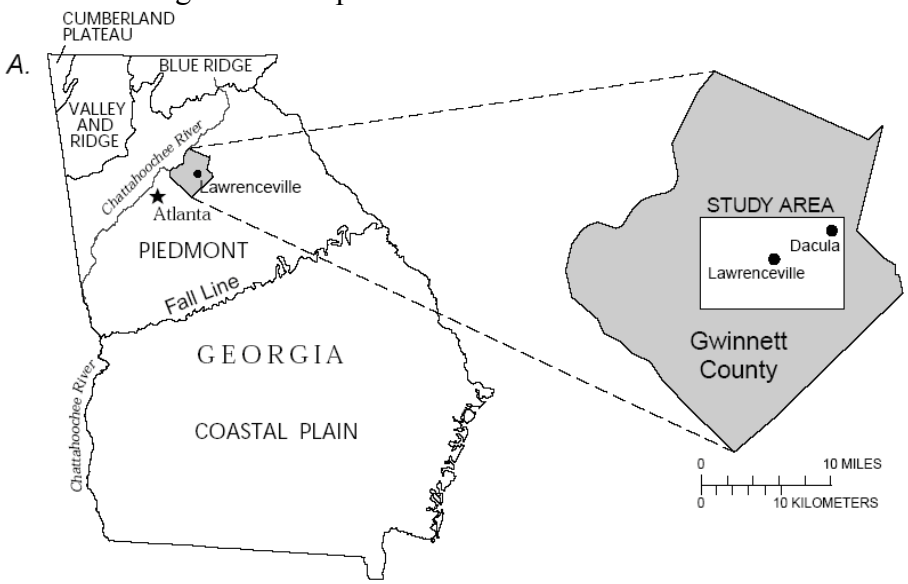

Figure 1. The Rhodes Jordan wellfield study area is located in Gwinnett County, GA. in the Piedmont Physiographic province (Figure from U.S. Geological Survey, Water Resources Division, Atlanta, GA)

The wells in the well field form a tight cluster downstream of the Lawrenceville City Lake (Figure 2). Multiple wells were drilled and studied for documentation of depth of joints. The jointing is typical of the crystalline Piedmont province. The joints sets are the conventional near-vertical orthogonal sets of joints with nearly horizontal stress release joints, which decrease in frequency with increased depth. The locations of the principal joints and their depths are identified in Figure 3.

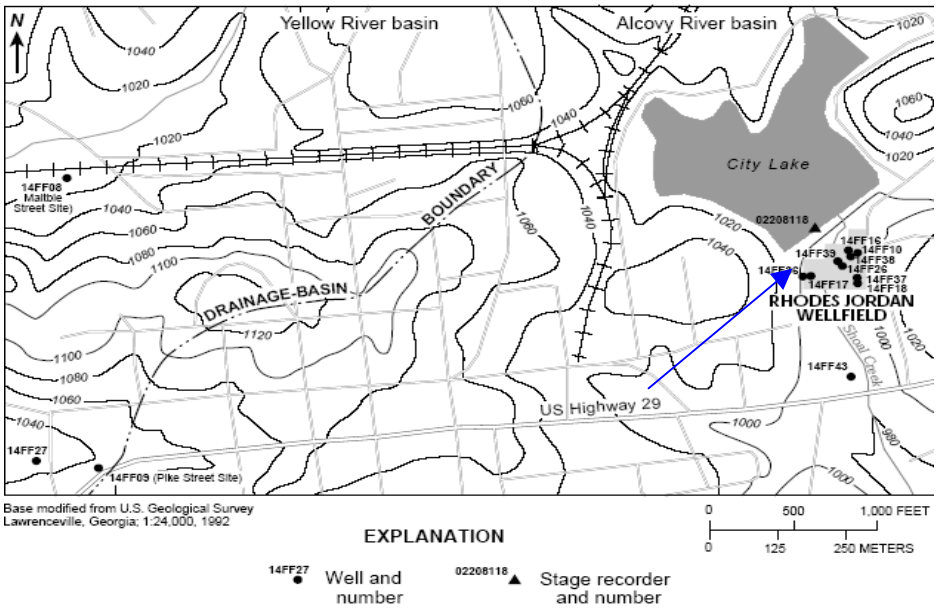

Figure 2. Observation wells in Lawrenceville, GA. The blue arrow poits towards the well which was used to deleniate fractures. (Figure from U.S. Geological Survey, Water Resources Division, Atlanta, GA)

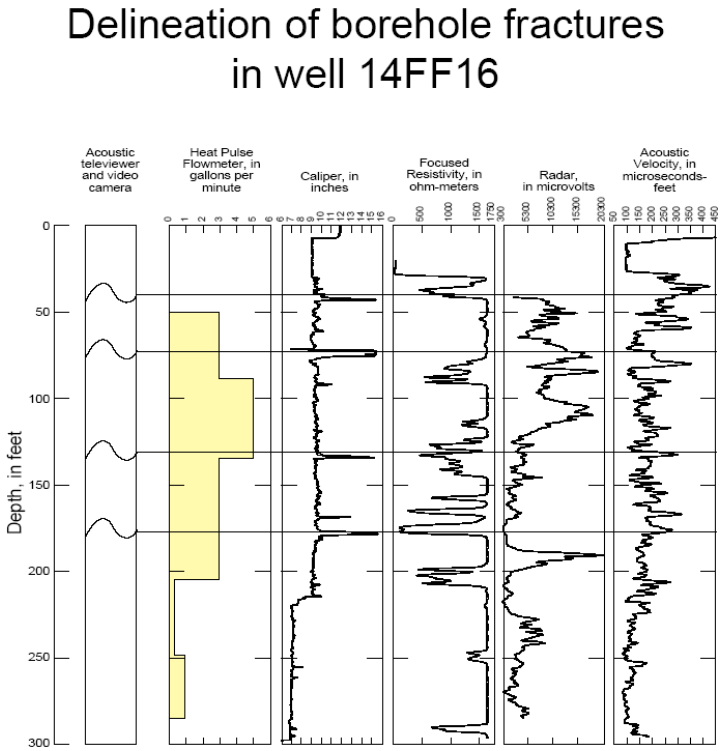

Figure 3. Delineation of fractures for well 14FF16. Two fractures were targeted in this study. First fracture is at 41.76ft (12.73m) and the second fracture is at 73.08ft (22.27m). (Figure from U.S. Geological Survey, Water Resources Division, Atlanta, GA)

Data analysis for shallow structure.

The seismic refraction technique was used to define the thickness of the soil layer. The data were collected in the fall of 2003. The geophones were spaced at 1 meter and the source was located a distance of 1m (at 4 meters) from first geophone. The travel times for direct and refracted waves are picked from the recorded seismograms and are shown on Figure 4.

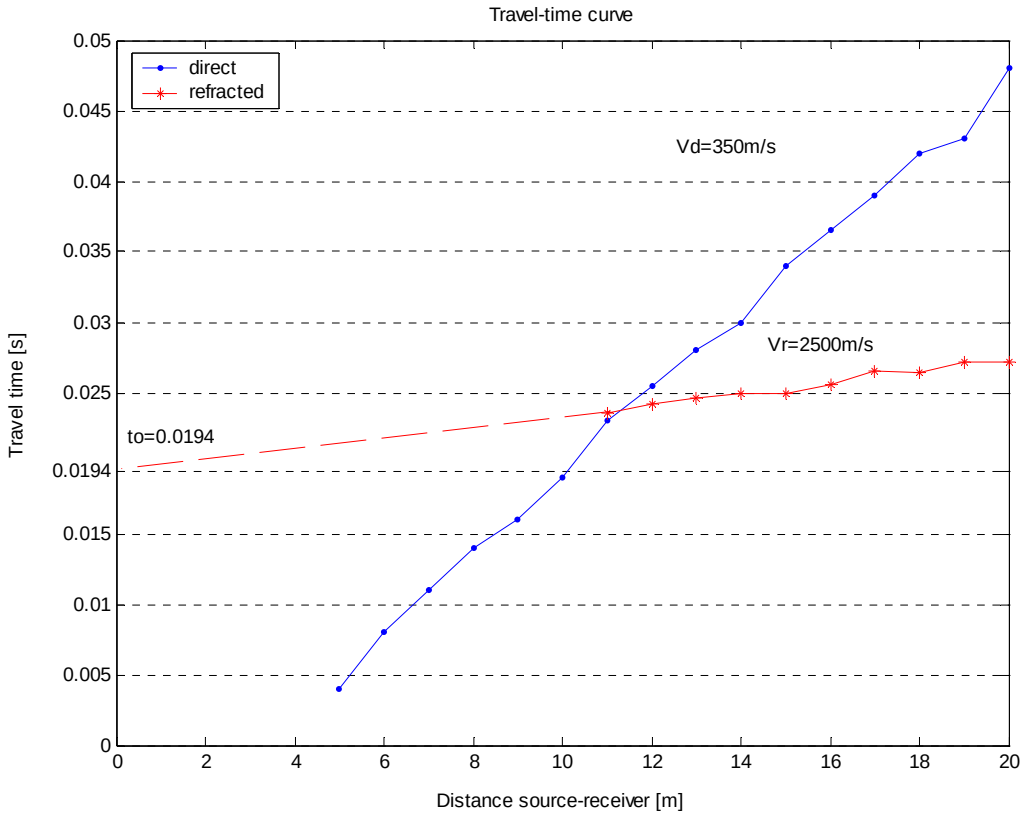

Figure 4. Travel time curves for direct and refracted wave. Velocities are calculated as the slopes of the two curves – $V_{direct}=V_{soil}=350$m/s and $V_{refracted}=V_{rock}=2500$m/s. The intercept time t_i is found to be 0.0194s. The computed depth to soil layer for this line is 3.4 m.

The depth of the soil layer was calculated from the equation:

$$h = \frac{t_o}{2}\frac{V_{rock}V_{soil}}{\sqrt{(V_{rock}^2 - V_{soil}^2)}} = 3.4\text{m}$$

We would expect there to be measurable variations in the thickness of the sediments, but do not believe this variation is sufficient to affect our results.

In order to obtain more information on the thickness of the sediments, we also performed a dispersion analysis of the surface waves. The observed dispersion for the data is shown on Figure 5.

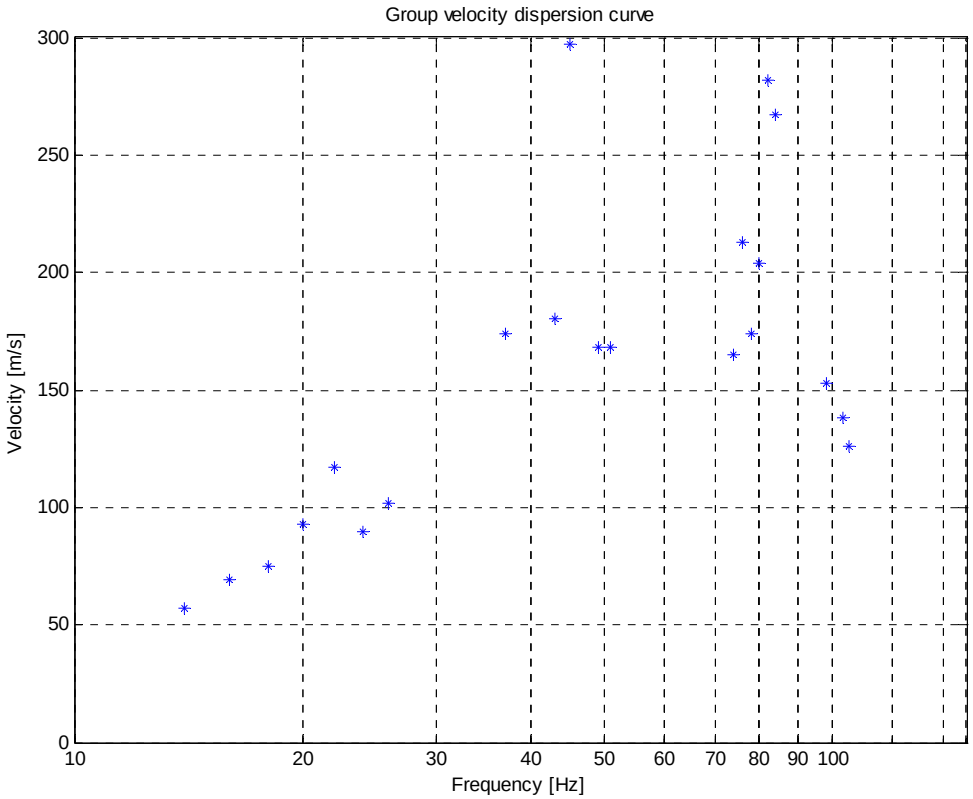

Figure 5. Observed group velocities of Rayleigh waves.

In order to find the structure, we used the forward modeling technique. In the forward modeling technique, a synthetic dispersion curve is found by varying the velocities and thicknesses of the soil until a fit to the observed data is found. The resulting velocity and layer structure is listed in Figure 6. The group velocity tends to increase with frequency, a phenomena often referred to as reversed dispersion. Reversed dispersion can be caused either by a low velocity zone at depth, by a sharp increase in velocity with depth, or both. In this case we were able to fit the dispersion curve with a structure with a low velocity zone and a sharp increase in velocity with depth. The low-velocity zone is very likely the depth of significant increase in water content. Also, the near surface soils contained many rock fragments suggesting that the surface had been reworked and likely contained a significant amount of unweathered crushed rock that could, in a dry packed condition lead to a higher near-surface velocity. These rocks in many cases made it difficult to plant the geophones because the spikes could not be pushed into the ground. The soil thickness of 3.5 m is approximately the same as that estimated from the refraction analysis.

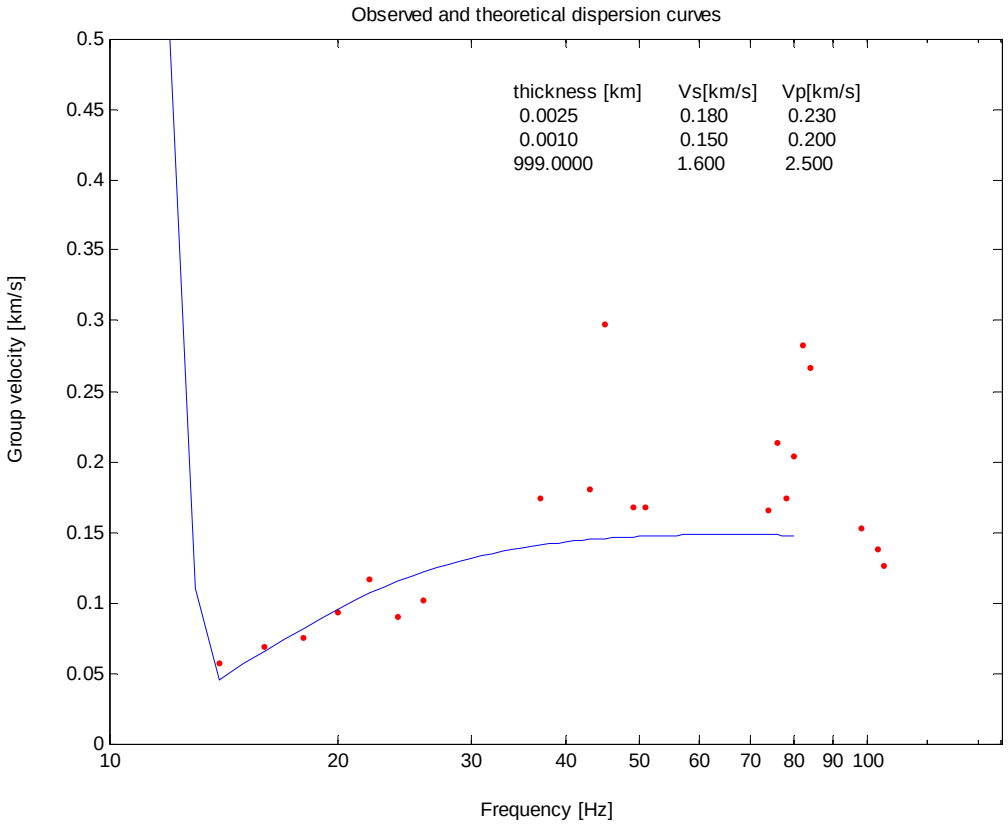

Figure 6. Observed (dots) and theoretical (line) dispersion curve.

Data Stacking for reflections

Data reduction in conventional seismic reflection processing includes the stacking of seismic traces that have reflected from the same reflector. In stacking, the time for the arrival from a given reflector is identified on each record trace and the traces are time shifted so that the reflection arrives at the same time on each trace and the traces are added. With proper time shift, the reflections on each trace will be coherent and will add, while noise and other reflections will be incoherent and tend to cancel out. The reflections are enhanced and made easier to identify.

In order to stack the traces on the expected times of the reflections from the fractures it is necessary to compute the expected times of the reflections. The times of the reflections increase with increased distance from the source. This is the normal move out, or NMO. Using the velocity profile defined by the refraction analysis, we calculated the NMO corrections for the fracture depths obtained from the down-hole well logs. The values assumes are; a soil velocity of V_{soil}=340m/s, a thickness of the soil layer h=3.4m, and a velocity of rock V_{rock}=2500m/s. With these data, the travel-time (Figure 7a) and the x^2-t^2 curve was generated (Figure 4b) for an assumed fracture depth of 12m.

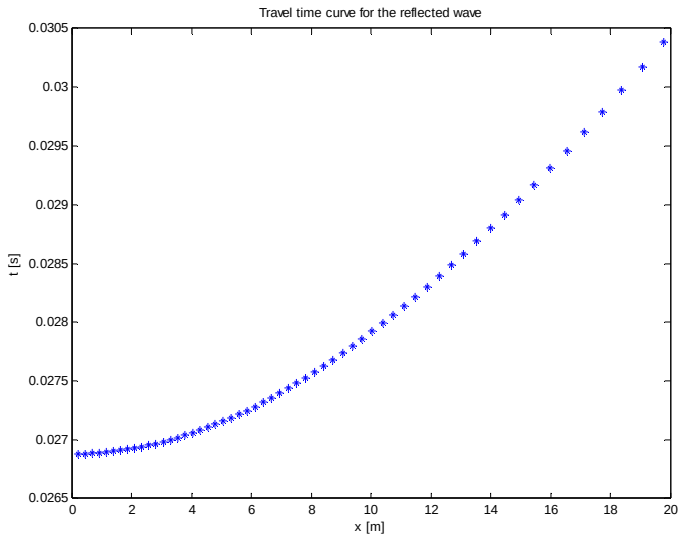

a)

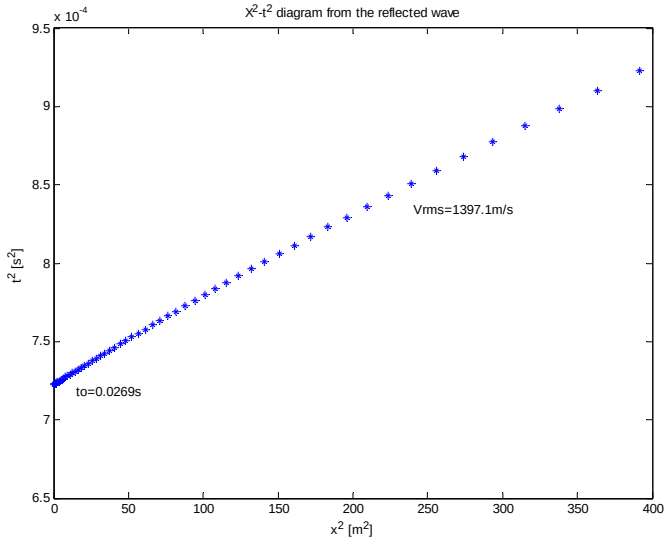

Figure 4. a) travel-time curve for the reflected wave; b) x^2-t^2 curve for the reflected wave. The rms velocity is defined to be 1397.1m/s and the intercept time is t_0=0.0269s.

The same computations were performed for the fracture at 23m and are shown in Figure 8.

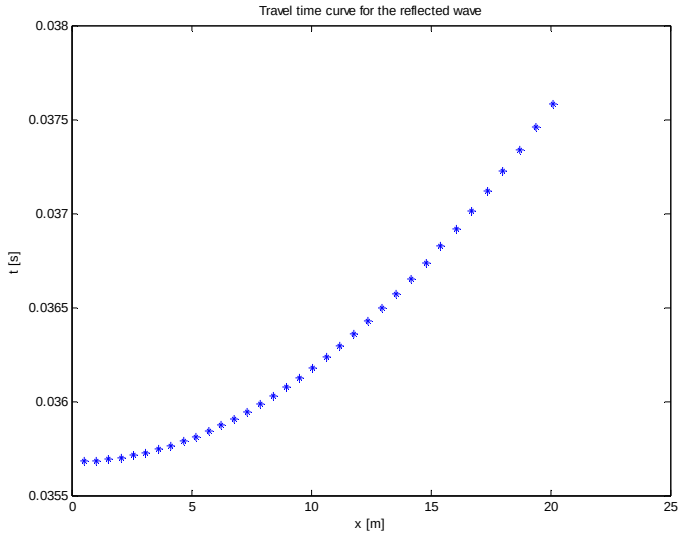

a)

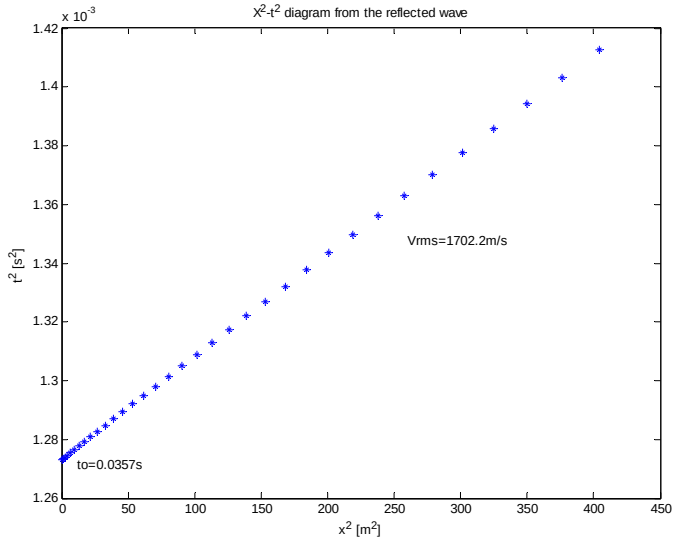

b)

Figure 8. a) travel-time curve for the reflected wave; b) x^2-t^2 curve for the reflected wave. The rms velocity is defined to be 1702.2m/a and the intercept time is t_0=0.0357s.

The computations were repeated again for the 40m fracture and the results are shown in Figure 8.

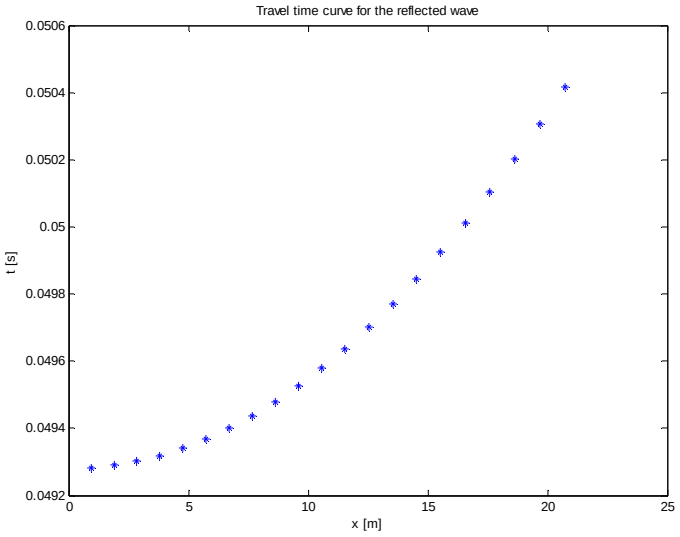

a)

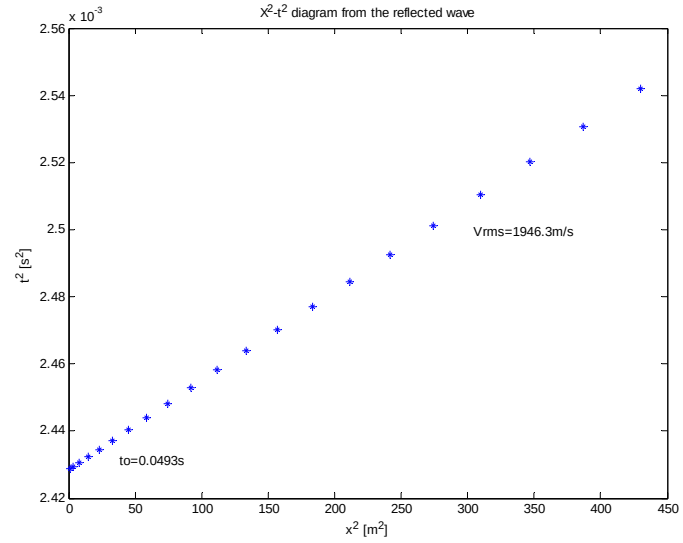

b)

Figure 9. a) travel-time curve for the reflected wave; b) x^2-t^2 curve for the reflected wave. The rms velocity is defined to be 1946.3m/s and the intercept time is t_0=0.0493s.

Arrival times were generated for the direct waves and reflected waves for the fractures at 12, 23, 40m depth in Figure 10a, Figure 10b, and Figure10c, respectively,

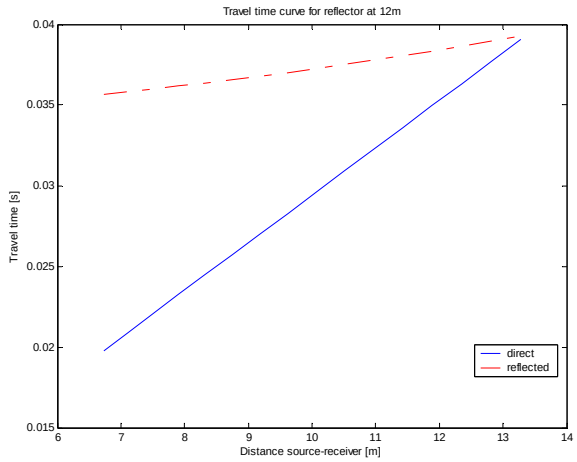

a)

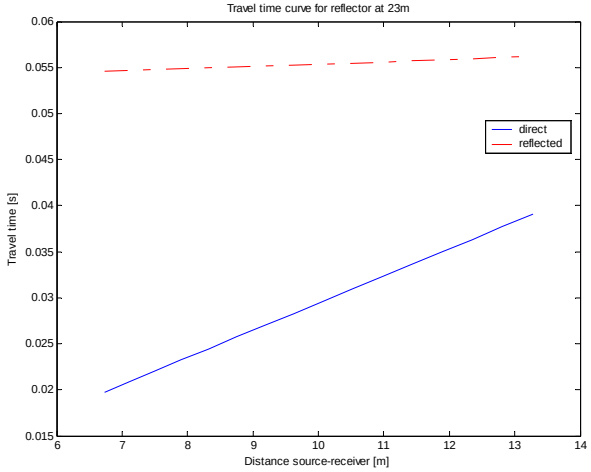

b)

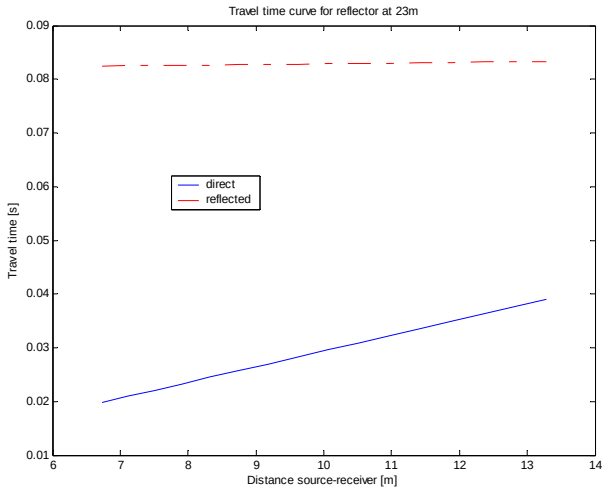

c)

Figure 10. Travel time curves for direct and reflected waves for a) 12m deep fracture; b) 23m deep fracture; c) 40m deep fracture.

The travel times in Figure 10 are the NMO corrections. These NMO corrections were applied to each trace and then the traces were added together. Figure 11a shows the original traces and their variation with distance from the shot. Figure 11b shows the traces after application of the NMO correction. Figure 11c is the stacked trace. The objective of stacking is to amplify coherent arrivals, the reflections, and cancel out non-coherent arrivals such as those from surface waves. The data in Figure 11 show the application of NMO for the 12m fracture. Figure 12 shows the application of NMO for the 23m fracture. Figure 13 shows the application of NMO for the 40m fracture.

The stacking was done for two wet records (during pumping) and two dry records (15min after pimping stopped). Comparison of records taken under similar conditions is a measure of the repeatability of our measurement of the seismic waves. Figure 14 shows how the amplitude of the stacked traces differs between dry and wet records. Figure 14 a shows the direct comparison of two shots before pumping and during wet conditions. Figure 14b shows the direct comparison of two shots when pumping had stopped, during dry conditions. Figure 14, shows a comparison of the seismic signal for wet and dry conditions. Because the comparison is not as great, we computed differences in the traces. Figure 14d shows the comparison of the differences in these traces. There is a clear difference in the traces with the difference exceeding twice the noise level as determined by differences between traces obtained under similar conditions. Figure 15 shows the repeat of the analysis for the fractures at 23m and 40m.

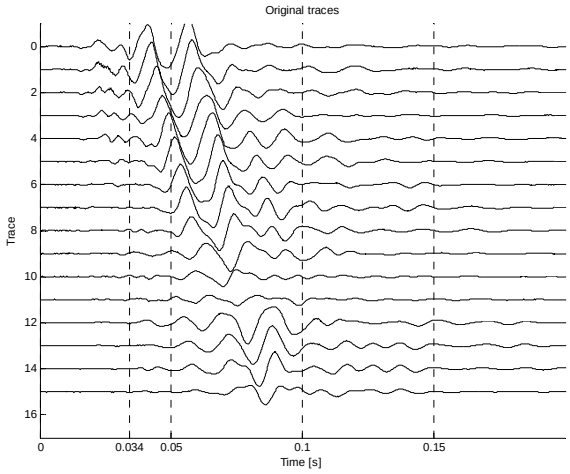

a)

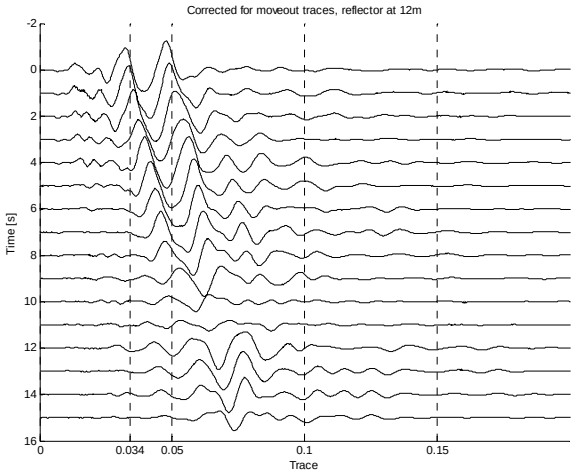

b)

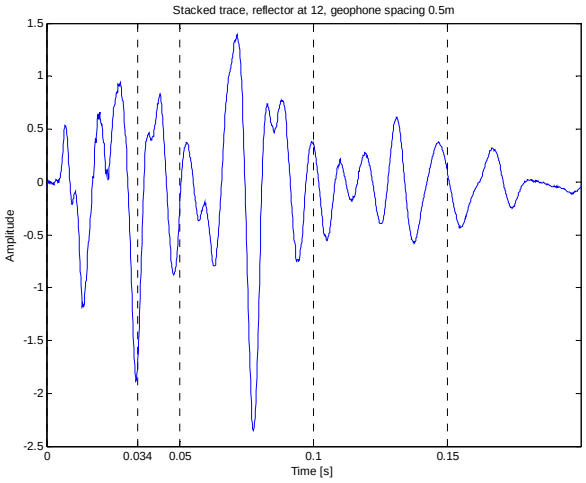

c)

Figure 11. a) original traces; b) corrected for nmo traces; c) stack trace, the fracture is nicely delineated at 0.034s.

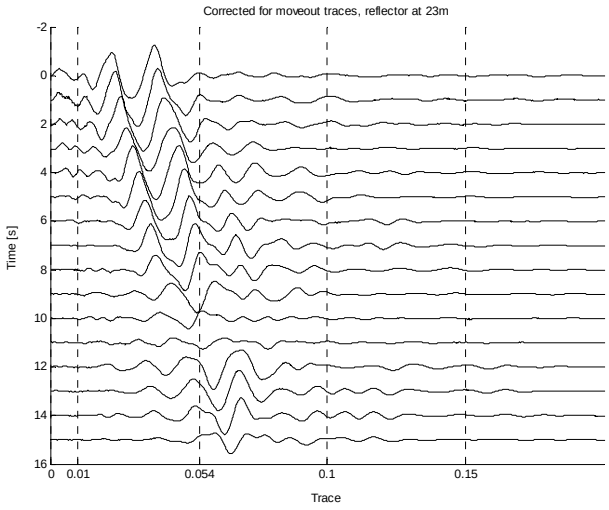

a)

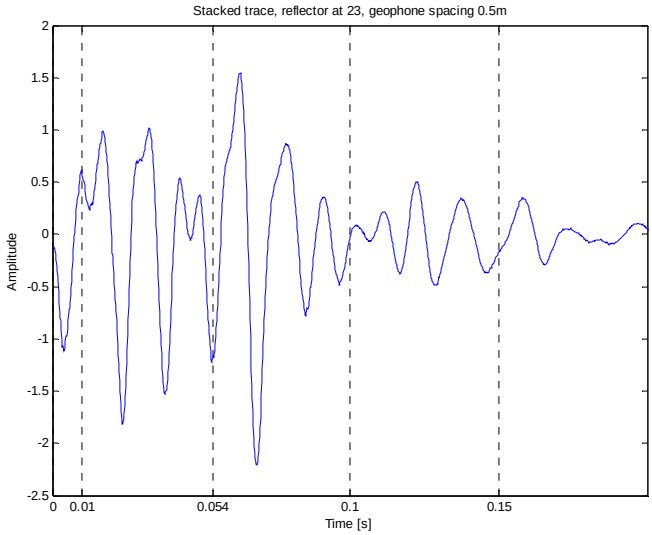

b)

Figure 12. a) NMO traces; b) stack trace delineates the fracture at 23m

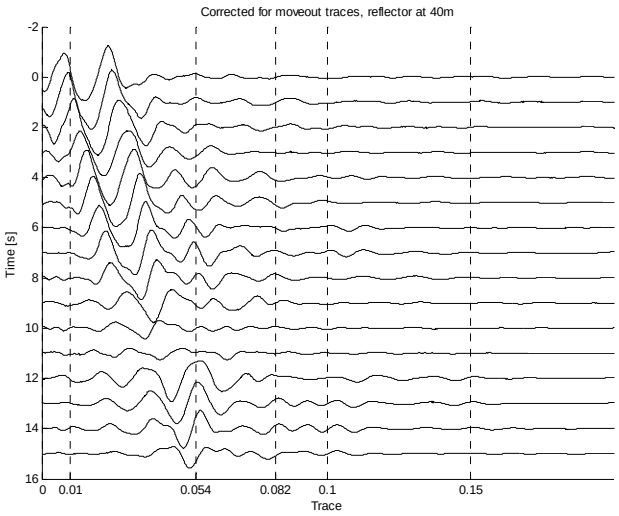

a)

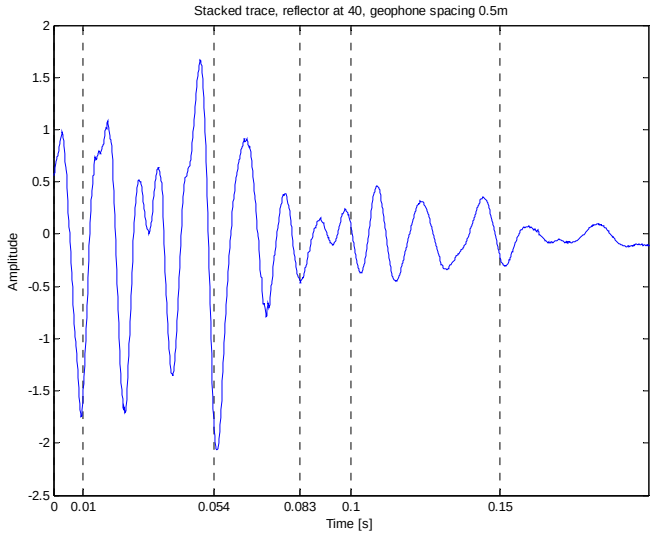

b)

Figure 13. a) NMO traces, b) stack trace, the 40m fracture is at 0.082s, although the reflection is quite weak. The 23m fracture is even more noticeable here.

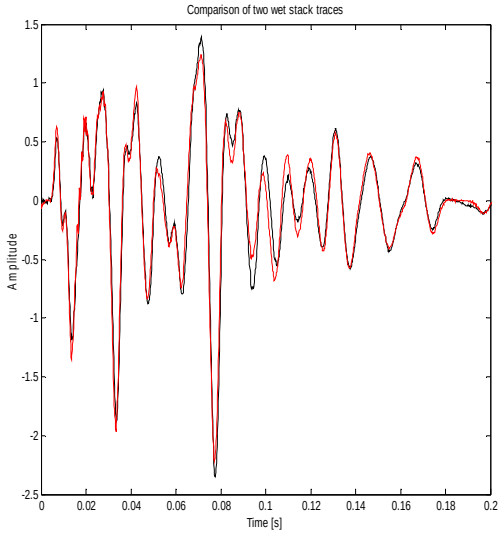

a)

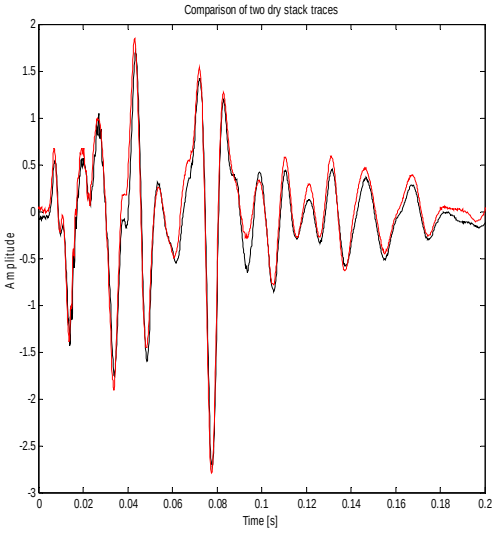

b)

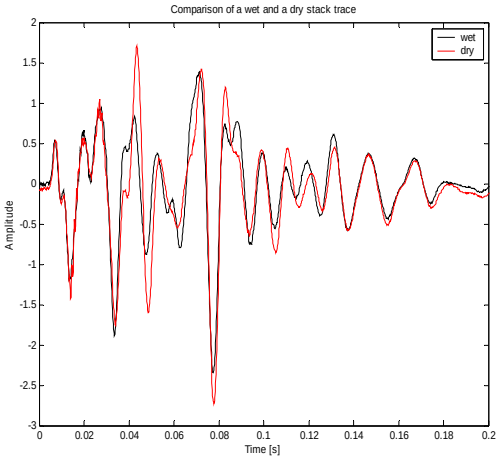

c)

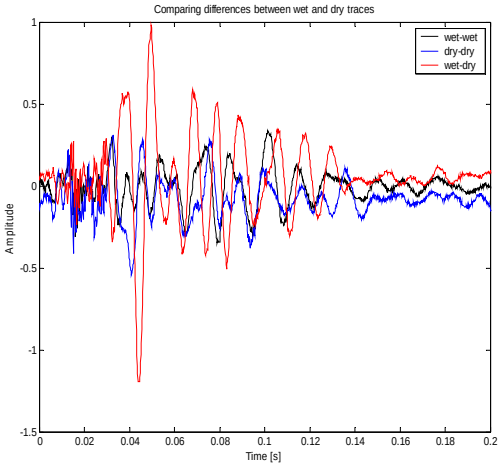

d)

Figure 14. Differential analysis for the 12m fracture. a) comparison of the stack trace of two wet records; b) comparison of the stack trace of two dry records; c) comparison of the stack trace of a wet and a dry records; d) comparison of the difference between two wet (black line), two dry (blue line) and a wet and a dry (red line) trace.

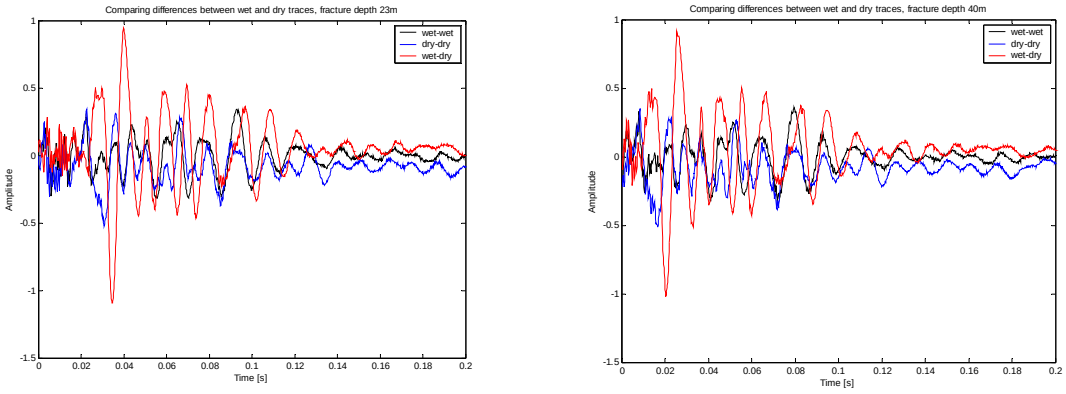

a) b)

Figure 15. Comparison of the differences between wet and dry records for a) 23m deep fracture; b) 40m deep fracture.

The resulting difference traces are similar, as might be expected because the move out functions are similar, but shifted in time. There is a distinct change in seismic properties under the different pumping conditions. It is not entirely clear that these changes are due to changes in the reflections from the fractures or to changes in water content in the shallow soil. More signal analysis may resolve the source of the anomalies.

Chapman, Melinda J. Thomas J. Crawford, and W. Todd Tharpe (1996). Geology and Ground-water Resources of the Lawrenceville area, Georgia, Water-Resources Investigations Report 98-4233, U.S. Geological Survey, Denver, CO, 56pp.

Appendix II

A Differential Approach for Detecting Temporal Changes in Near-Surface Earth Layers

Based on the presentation by Tatiana Toteva, and L.T. Long, at the 76th Annual Meeting, Eastern Section Seismological Society of America, Virginia Polytechnic Institute and State University, Blacksburg, Virginia. October 31 to November 1, 2004.

Abstract: The physical parameters (shear wave velocity, density, porosity, etc.) of near-surface soils and weathered rocks have been extensively studied for the purposes of geotechnical engineering, hydrology, oil and gas exploration etc. The possibility of using geophysical techniques for monitoring changes within this upper layer has gained big popularity within the recent years. The objective of this study is to develop a differential technique for detecting subtly velocity changes within the soil layer. The differential technique is based on a study of the difference between two normalized traces taken at successive time intervals. The differences are interpreted as perturbations to a structure. This study has applied the differential technique to Rayleigh waves. We hypothesized that fluid penetration due to natural causes (rainfall) or pumping of fluids, would lead to changes in the shear wave velocity, which could be detected on the differential seismograms. In the traditional approach the soil layer is studied by inverting the phase velocity dispersion curve for the velocity structure. Instead of the phase velocity we use group velocity for inversion curve. Group velocity depends on phase velocity and the change of the phase velocity with frequency. Hence, we hypothesized that group velocity would be more sensitive to subtle changes in the velocity structure. The technique was tested for two different types of soil perturbations. We acquired data before and after heavy rain in the Panola Mountain Research Watershed to test the effect of variations in water table and soil moisture. At a second site, we tested a more controlled perturbation by pumping water into the soil at a depth of about 1.0 meter. Important factors in the acquisition of this data were the use of a repeatable weight-drop source and a secure and repeatable geophone placement. Our results show that the fluid penetration I the soil causes phase changes and time shifts, detectable on the differential seismograms.

Introduction

The objective of this study is to demonstrate a differential technique for detecting subtle velocity changes, particularly those occurring within the near-surface soil layer. We hypothesized that fluid penetration due to natural causes (rainfall) or the pumping of fluids would lead to changes in the shear wave velocity, which in turn could be detected by the group velocity dispersion curve. Subtle changes in seismic velocity can be expressed as subtle time shifts in seismograms. Hence, we obtain seismic data with the same source and receiver positions at sequential times in order to monitor the change in velocity.

Surface Wave Analysis:

Conventional surface wave analysis uses either the phase velocity or group velocity to determine the dispersion curve in a specific area. In this study, we will do this along a line, obtaining dispersion relations for phase and/or group velocity as a function of position along the line. The standard procedure is to use the dispersion relation to find a layered velocity structure under the area with the dispersion curve.

Instead of mapping variations in structure (note, the structure could be provided as a separate analysis) in differential surface-wave interpretation we look for time variations in the dispersion curves (as indicated by time variations in the seismic trace) induced by changes in

fluid content. The reference or average structure is no longer critical to the analysis so long as a reasonable approximation is available to generate appropriate theoretical differences in dispersion induced by known perturbations in the structure. For the differential approach, the reference is not the pre-test velocity structure, which is generally unknown in detail, but is the seismic trace from the unperturbed structure, which is available from an earlier survey. In the differential approach, we measure the differences in the dispersion for waves traveling the same path by direct comparison of two seismic traces recorded at different times. The direct comparison gives the time shift.

The time shift between two phases can be expressed as the difference between the phases of the two traces by the equation,

$$\delta t = \frac{\Delta \varphi}{2 \pi f}$$

where for angles less than 45 degrees,

$$\Delta\varphi = \sin^{-1}\left(\frac{A_{ref} - A}{A}\right)$$

and the A's are the amplitudes of the reference trace and the perturbed trace.

Data for this study were collected at the Panola Mountain Research Watershed using 15 Hz geophones on the established line. A linear array of geophones with one meter spacing was used for the recording of the data. The line was marked with permanent concrete geophone mounts. The data taken after each hurricane represent wet saturated ground. The weight-drop source was placed 5m from the first geophone. Measurements were taken before and one day after each of two major hurricanes –hurricane Frances and hurricane Jeane. On comparison (Figure 1.) the phase arrival times look similar for the two events.

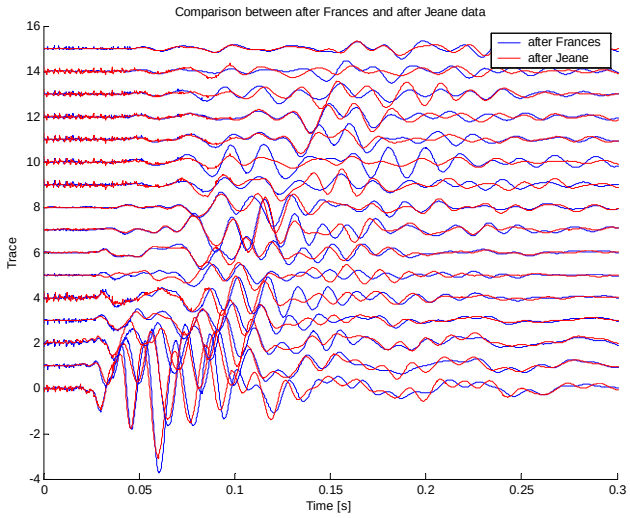

Figure 1. Comparison of data recorded during wet periods after two storms.

However, in Figure 1, the amplitudes vary along the line. In contrast, both the amplitudes and the phases appear to vary when comparing data between dry and wet periods (Figure 2).

Figure 2. Comparison between records recorded during dry periods before the storms and wet

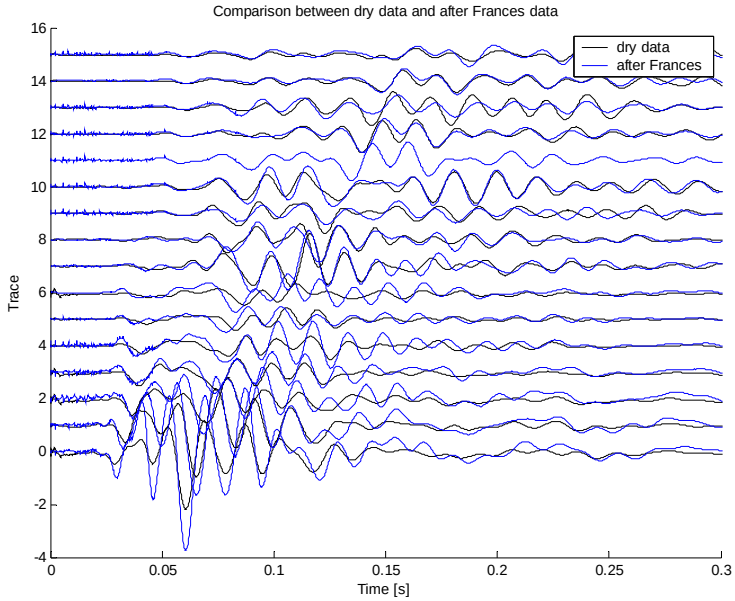

period after the storms.

In all tests we showed that the tests over a short time period were repeatable, giving in all cases almost identical signatures. The differences represent variations in the velocity structure with time. In order to quantify these changes, we have computed group velocities from the data and for filtered data we have computed the phase shifts. The group velocities are shown in figure 3. In the 20 to 30 Hertz range, which is appropriate for a reasonable sampling of the top meter of soil and rock, the velocities following the two hurricanes were distinctly lower. Reduced velocity would be expected for the increased density associated with a higher water table

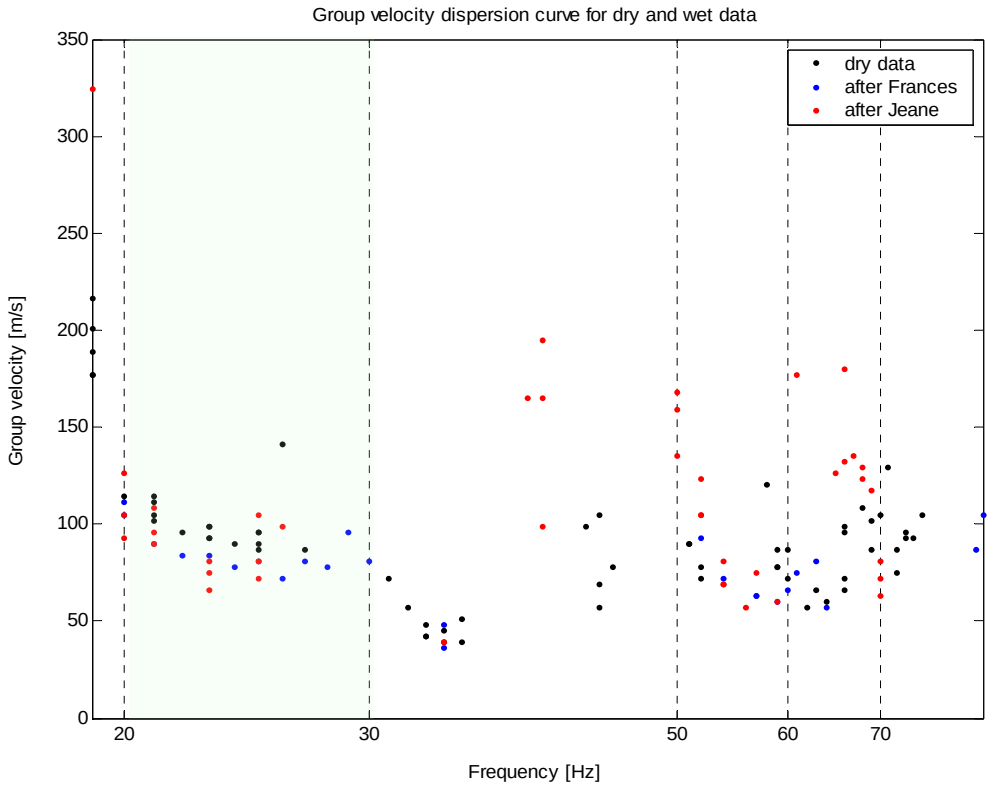

Figure 3. Group velocities observed before and after major storms and associated changes in water saturation.

In order to compute actual changes in arrival times for particular phases, we used a multiple filter technique. The filtered data for 30 Hz is shown in Figure 4. The traces showed that the amplitudes were higher when water content was higher than they were during dry periods. While the phase shifts for the hurricane data were similar, there were significant shifts in phase relative to the dry recording periods. Figure 5 shows the computed time differences in the arrival of various phases. The reference is the record during the dry period. The dry trace line in Figure 5 indicates that the source is stable in the first half of the line and becomes increasingly unstable at the most distant geophones. The progressive increase in time in the short distances, with increasing times with distance, suggests that the velocity has been reduced by increased water content. The velocity decrease amounts to about 5 percent.

Conclusions

The very good repeatability of the source allows detection of subtle time shifts in dispersed surface waves. In particular, soils with higher water content, such as following a significant rain event, have lower group velocity than data obtained when the soils are dry. We were able to detect time differences comparable to the sampling interval by measuring the phase shift defined over a few cycles of wave motion.

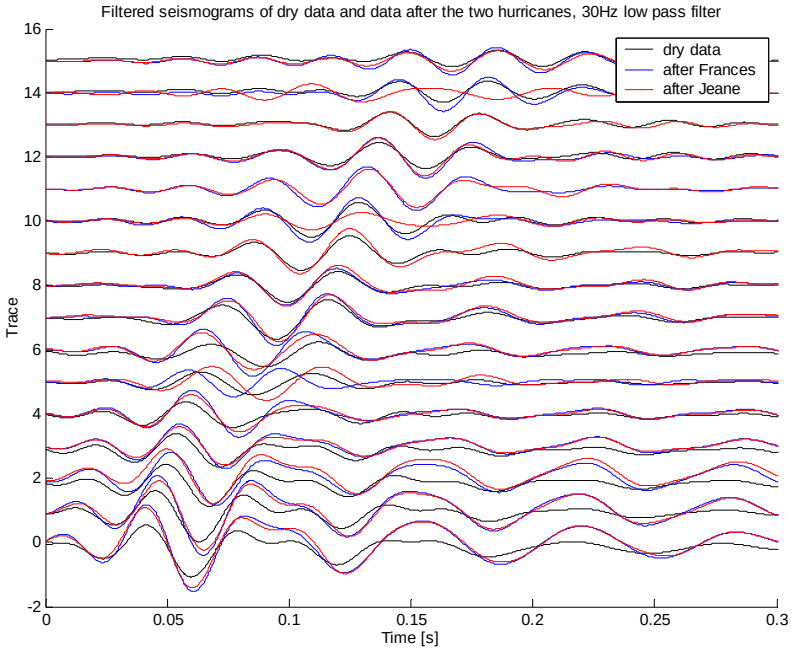

Figure 4. Data filtered at 30 Hertz showing comparison of data during dry periods and following hurricanes Frances and Jeane.

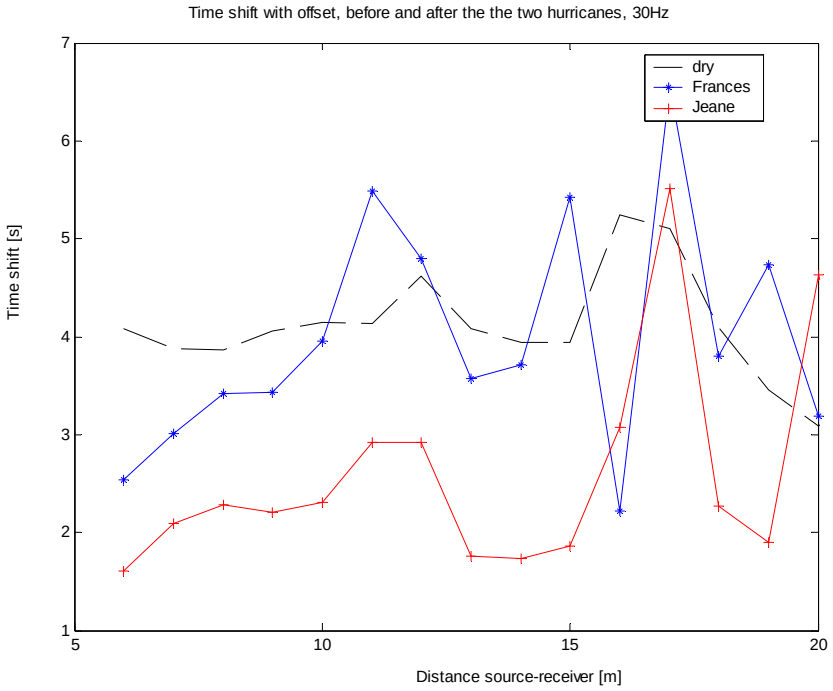

Figure 5. Computed time shifts for 30 Hertz.

Appendix III

A scattering inversion experiment to identify fractures on a granite outcrop

Tatiana Toteva and L. T. Long.

Abstract: A critical need in understanding open or fluid filled fractures in crystalline rock is the ability to identify these fractures, to characterize their source zones, to map flow paths within the fractures, and to assess residence time of water in the system. Fractures are an important component in the water resources of areas where crystalline rocks crop out at the surface. We have attempted to use scattered waves to identify and map fractures in a crystalline rock. Our research was conducted at the Panola Mountain Research Watershed (PMRW), GA. The scattering technique was tested in an area of exposed rock. We used 16 geophones placed in a circular array with diameter of 16m. The free period of the geophones is 100Hz. A major effort was taken towards suppressing resonances of the geophones at high frequency. We used clay to better attach the geophones to the outcrop and sand bags to weight the instruments down to suppress the high frequency resonance. A small weight-drop source was designed to generate a high-frequency input signal. The source provided signals in the 300 to 800 Hz range. The source was moved to shot points in the distance range of 5 to 60 meters from the recording array. The recorded signals were high-pass filtered to allow only waves above 500 Hz. Analysis of the data gave independent estimates of the velocities of surface waves on the rock and shear and compressional wave velocities in the rock. In processing the data, the distance of travel of a scattered wave was obtained from the travel time. The direction to the scattering fracture is obtained by interpreting maximum the semblance as a function of apparent velocity and direction of propagation. The technique provides a theoretical way to map positions of varying scattering efficiency and hence the location of fractures.

Introduction to scattering inversion for fracture detection

Scattering inversion is a form of the 3-dimensional migration used in processing seismic reflection data in industry. The basis for the scattering inversion we propose has been described in detail by Chen and Long, (2000a). By combining a two dimensional array of geophones and sources, the sites of reflections can be located in a 3 dimensional spatial grid. As in the study by Chen and Long (2000a) the inversion can be improved by performing the stacking by using the Algebraic Reconstruction Technique (ART). However, in this study we have used beam focusing with an array of geophones to give the direction of arrival of scattered waves. This refinement to the Algebraic Reconstruction Technique is a significant improvement because it strongly limits the source zone of the reflection.

Summary of scattering inversion: The generally accepted model for the seismic coda is a superposition of wavelets scattered back from many structures (Aki, 1969, Aki and Chouet 1975). This coda model has been refined in order to relate coda decay to the scattering and attenuation properties of the earth's crust (Sato, 1977; Frankel and Wennerberg, 1987; Revenaugh, 2000). A fundamental assumption of the coda model is that intrinsic absorption and

the distribution of structures causing scattering is uniform. As a result of this assumption, all these models predict that the seismic coda should decay smoothly and that the coda decay rate should be independent of the hypocenter. However, in most recordings of seismic events the rate of decay deviates from this prediction. As is well known from reflection seismic methods, the seismic coda does not always decay smoothly, often containing anomalous amplitudes from waves reflected from structures at depth. These observations suggest that the assumptions concerning the uniform distribution of structures that scattered wave energy or the uniform distribution of intrinsic absorption may be violated. This conclusion should have been expected because the structures that scatter seismic energy are rarely distributed uniformly in the earth's crust. For example, open fractures that can scatter significant seismic energy are clustered near fault zones and are more prevalent at shallow depths where the lithostatic pressure is too low to close joints or fractures.

In the past decade, several studies have attempted to characterize the distribution of structures that scatter seismic waves. One approach is to apply frequency-wavenumber (F-K) analysis to the data from dense seismic arrays (e.g. Furumoto *et al*., 1990). Studies based on this approach have identified waves scattered from geological structures and topographic relief near the recording stations. Our approach is the coda envelope inversion technique (Ogilvie, 1988; Nishigami, 1997; Chen and Long, 2000a, Revenaugh, 2000). One advantage of this approach over the F-K analysis is that coda envelope inversion does not require a dense array of stations. An advantage over the Kirchhoff depth-imaging method (Sun et al., 2000) is the reduction in required data processing. Coda envelope inversion is appropriate when the coda is long compared to the period of the waves. For shallow scattering, Kirchhoff depth imaging methods may be required. Part of this research is to define the conditions under which Kirchhoff migration and coda envelope inversion techniques work best.

The effectiveness of coda envelope inversion can be illustrated by results from Chen and Long (2000a). Figure 3 shows the distribution of scattering coefficients surrounding the Norris Lake Community seismicity. The epicenters of the many earthquakes of this swarm are located near the center of the image. The 5 to 7 stations recording the small earthquakes surround the epicentral zone.

The areas of greater relative scattering coefficients are closely associated with the epicentral zone in the center, and near some geologic structures along the east border of the image area. The distribution relative scattering coefficients showed that fracture density decreased rapidly with depth. One important observation is that the shallow scattering coefficients are strongly frequency dependent, indicating scattering from fractures rather than from velocity contrasts that would be frequency dependent.

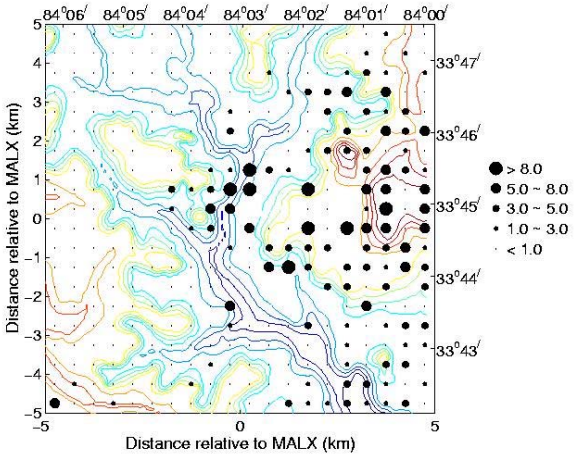

Figure 3. Relative scattering coefficients at 17 Hz for a depth of 0.25 km.

The theoretical model for the scattered waves in the coda is given in the paper by Chen and Long (2000a) and can be summarized as follows. The coda energy level at lapse time *t* is a function of the source radiation pattern, the numerous velocity anomalies and discontinuities that scatter seismic energy, and the propagation properties of the medium. Most investigations (Aki and Chouet, 1975; Sato, 1977) assume that the propagation may be represented by statistical methods. To obtain information about a non-uniform distribution of scattering coefficients, deterministic methods such as those of Ogilvie (1988), and Nishigami (1997) must be used. In the coda envelope inversion of this study, we take advantage of the simple expressions of the statistical method to find the master curve of coda decay. Then a deterministic method is used to find the scattering strength of individual structures relative to the master curve of coda decay. Relative scattering coefficients are the ratio of the actual scattering coefficient of a scattering structure to the average scattering coefficient of the region. In statistical methods, uniform and random distributions of scattering structures, spherical radiation of energy from the source, isotropic scattering and homogeneous velocity structure are usually assumed. Furthermore, if the scattering does not contain converted phases, and the medium takes up the whole three-dimensional space, then the mean energy density of scattered waves at frequency ω can be found by the single isotropic scattering theory of Sato (1977),

$$E_0(r,t \mid \omega) = \frac{Wg_0}{4\pi V^2 t^2} K(\frac{t}{t_s}) \exp(-\frac{\omega t}{Q_c}) \qquad (1)$$

where W is the total energy radiated from the source at frequency ω, g_0 is the average scattering coefficient of the random medium, Q_c is the coda quality factor, V is the velocity of the S wave, t is the lapse time of coda waves measured from the earthquake origin, t_s is the travel time of direct S wave, and $K(t/t_S)=(t_S/t)\ln[(t+t_S)/(t-t_S)]$. Here we put a subscript 0 for both E and g to denote that both parameters hold the average value and that they are derived for a uniform distribution of scattering objects.

From the deterministic point of view, the medium consists of discrete scattering structures at defined locations. If the phases of scattered waves are randomly distributed, we may assume that the scattered waves can be regarded as incoherent. Then, the energy of the scattered waves contained within the lapse time window [t_j-δt/2, t_j+δt/2] will be equal to the summation of the individually scattered waves arriving within this window. In a constant-velocity medium the scattered waves that meet this travel time condition are contained in an ellipsoidal shell whose foci are located at the source and receiver. For a source and receiver in close proximity, the shell is approximated by a sphere whose inner radius is $V(t_j-\delta t)/2$, and whose thickness is $V\delta t/2$. If the scattering cross section of each scattering structure takes the average value σ_0, and if the total number of scattering structures falling into the shell is N_j, then the energy contained in the lapse time window [t_j-δt/2, t_j+δt/2] is approximated (Aki and Chouet, 1975; Sato, 1977) by,

$$E_0(t_j)\delta t = \frac{WN_j\sigma_0}{(4\pi)^2(Vt_j)^4}\exp(-\frac{\omega t_j}{Q_c}) \qquad (2)$$

For the uniform distribution of scattering coefficients and the homogeneous distribution of Q_C, equation (2) predicts that the coda wave amplitude will decay smoothly with lapse time and be random. However, fluctuations in the coda decay are caused by the non-uniform distribution of scattering coefficient and/or intrinsic absorption. For a non-uniform distribution of scattering cross sections, we assume that the scattering cross section of each structure is unique. In this case, the scattering cross section for structure *i* can be written as $\sigma_i=\chi_i\sigma_0$, where χ_i is called the relative scattering coefficient. The energy contained in the coda waves in a lapse time window becomes

$$E(t_j)\delta t = \frac{W\sigma_0}{(4\pi)^2(Vt_j)^4}\exp(-\frac{\omega t_j}{Q_c})\sum_{i=1}^{N_j}\chi_i \qquad (3)$$

Here the relative scattering coefficient χ_i measures the ratio of the scattering strength of an individual scattering object to the average scattering strength of the medium.

Following the method of Nishigami (1997) and divided equation (3) by equation (2), we finally get

$$\frac{E(t_j)}{E_0(t_j)} = \frac{1}{N_j}\sum_{1}^{N_j}\chi_i \qquad (4)$$

Equation (4) indicates that the ratio of observed energy density displayed in individual coda to the average energy density is independent of the source response and path effects. Also, equation (4) indicates that the ratio is equal to the average of the relative scattering coefficients of those structures responsible for the generation of this part of the coda.

For each seismogram, the coda is divided into small time windows, each of which gives an equation based on equation (4). For these equations, the scattering objects contributing to each time window are contained in a series of ellipsoidal shells. The number of scatterers can be large, over 13500 in the Chen and Long (2000a) study. Equation 4 leads to a very large but sparse matrix.

For monitoring the change in scattering coefficients from fractures (4) should be modified by replacing the vector of the ratio $e_j=E(t_j)/E_0(t_j)$ with its change δe_j and the vector of the relative scattering coefficients with $\Delta\chi_i$.

The coda-envelope-inversion is conventional tomography, in which conventional matrix inversion methods are not practical. In this study, the iterative Algebraic Reconstruction Technique (ART) is used to find a solution for equation (4) (Humphreys *et al*., 1984; Nakanishi, 1985). We first make an arbitrary initial guess at the solution. In this study we assign a value of one to all χ_i's so that the initial solution represents average background level of scattering coefficients. We examined other starting solutions but found that we obtained the same solution for each. We applied a relaxation parameter to control the rate of convergence and a constraint that all relative scattering coefficients remain positive. In this formulation successive iterations of the ART algorithm converge to a constrained and damped least square error solution (Kak and Slaney, 1988, pp280-281). In our study, the relaxation parameter was given a value of 0.1 and the iterations were truncated when the model parameters change less than 5% for additional iterations.

The use of an array of geophones provides a significant advantage in performing the scattering inversion. The array can be analyzed for velocity and direction of approach of the scattered waves by computing the semblance for an array of apparent velocities and directions.. Semblance is a measure of multichannel coherence. Semblance is computed from

$$S(t)=\frac{\sum_{j=t-N/2}^{t+N/2}\left[\sum_{i=1}^{M}F_{ij}\right]^2}{M\sum_{j=t-N/2}^{t+N/2}\sum_{i=1}^{M}\left(f_{ij}\right)^2}$$

where M channels are summed. The coefficient for time t is evaluated for a window of width N. The time at the center of the window, t, is adjusted for each trace to correspond to a direction of approach and apparent velocity across the array. An example of semblance analysis for one shot at the PMRW is shown in Figure 4.

Figure 4 is a plot of semblance as a function of apparent velocity and angle of approach. The arrival of surface waves, shear waves and compresional waves is indicated by high semblances at appropriate velocities. The surface waves show consistent peaks at velocities near 2300m/s. The surface of the granite is relatively unweathered and the surface waves do not show significant dispersion. This condition is a clear advantage for recording scattered waves because there are no dispersed surface waves to interfere with the scattered waves. For both the compressonal and shear waves, the apparent velocity varies, depending on the angle of emergence. The angle of emergence is the angle between the ray path and the horizontal. The angle of emergence for shear waves varies from 0 degrees (horizontal propagating waves) at the shear wave velocity of about 3200m/s to about 55 degrees at the compressional wave velocity of 5500m/s. The compressional wave arrivals show velocities of 5500m/s or above, depending on angle on their angle of emergence. There are apparent velocities in the range of 5500m/s and above where both shear and compressional waves can give measurable semblances. However, shear waves at near vertical angles of emergence are not recorded strongly on vertical seismometers and the near vertical compressional waves would be expected to be strong arrivals

on the vertical geophones. We have assumed that the waves travel their entire path as either surface waves, shear waves or compressional waves. It is very likely that some portion of the arrivals at the array represent converted waves. That is, waves that start as a shear wave and on reflection at a fracture are converted to compressional waves and detected as compressional waves at the array. These are fortunately not coherent and would not accumulate at one reflection location as a strong reflection. Hence, converted waves may contribute to the noise background, but would not interfere with the detection of fractures.

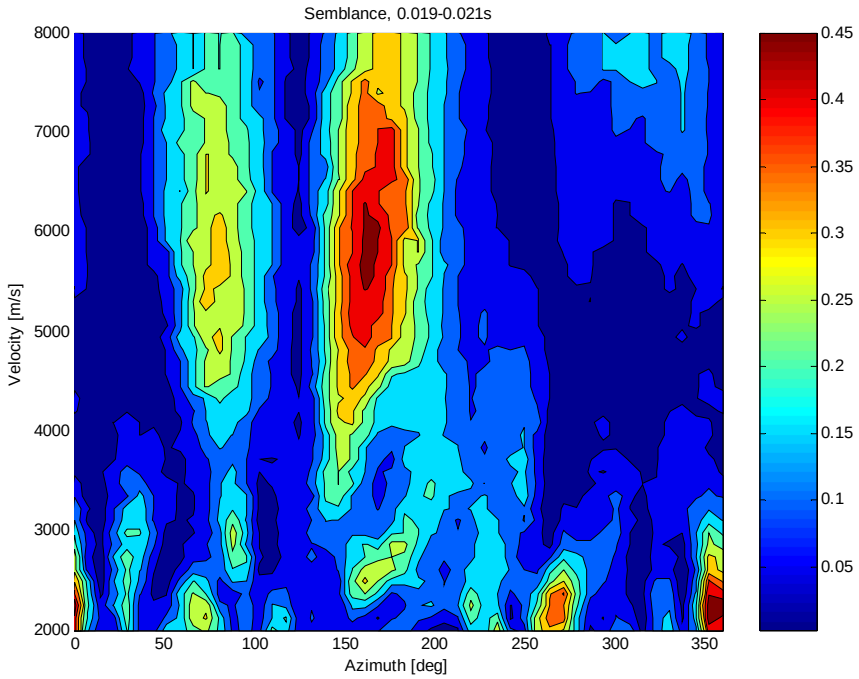

Figure 4. is a semblance plot showing a strong compresional wave arrival at 160 degrees. A shear wave arraival can be seen at 90 degrees and surface wave arrivals appear at 70, 270, and 360 degrees.

Because the semblance plots give tightly constrained angles of approach for both compressional and shear waves, iteration with the ART algorithm is not needed to locate fractures. Iteration would be needed to quantify the strength of scattering from the fracture. In this analysis we have computed the semblance for multiple times in the coda for about 14 shot point locations on the granite. The 14 shot point locations were in the shape of a rectangle. In order to test the imaging program and its ability to locate sources of signals, we applied it to the time window containing the direct surface wave arrival. The surface wave arrival should point back to the origin, and correspond to the shot point. The results of this first test are shown in Figure 5. The only shot points not clearly imaged are those on the left in Figure 5. The background noise appears as circles surrounding the origin of the recording array.

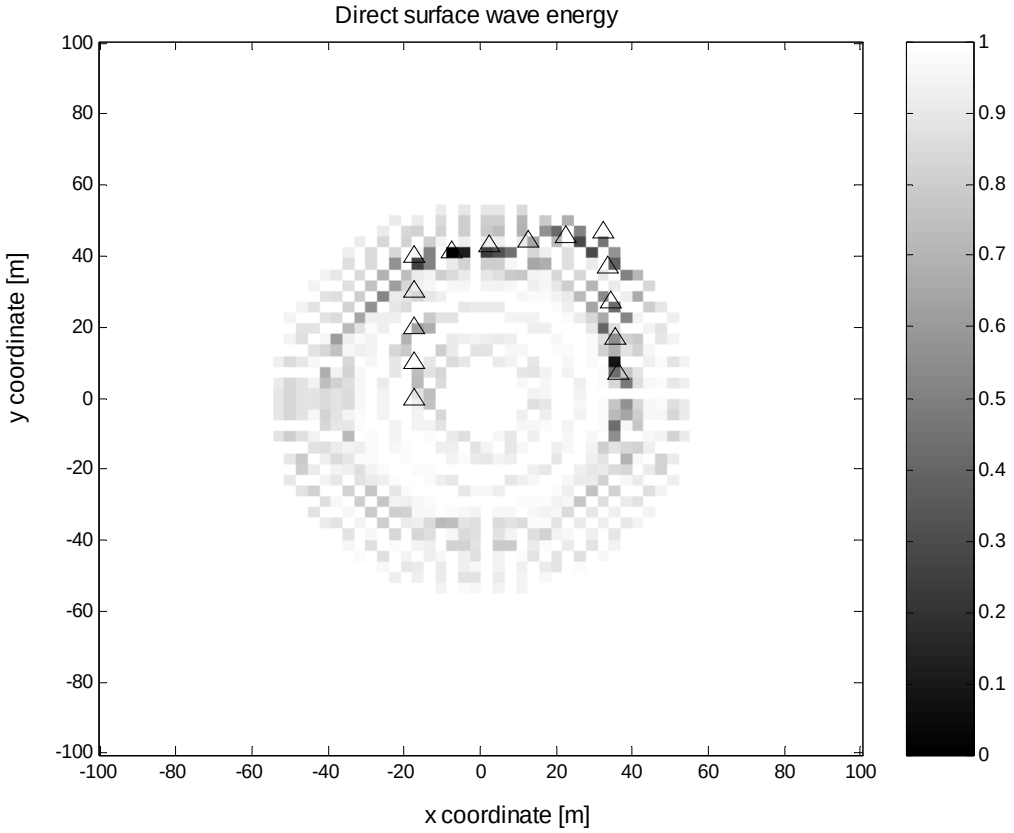

Figure 5. Inversion for sources using only windows in the arrival time of the surface wave. The triangles show the actual locations of the shots, the bright squares, particularly those on the top and right, are indicated sources of the signals.

Bibliography

Aki, K.(1969). Analysis of the seismic coda of local earthquakes as scattered waves, *J. Geophys. Res.,* **74**, 615-631.

Aki, K. and B. Chouet (1975). Origin of coda waves: source, attenuation and scattering effects. *Journal of Geophysical Research*, **80**, 3322-3342.

Chen, Xiuqi, and L.T. Long (2000a). Spatial distribution of relative scattering coefficients determined from microearthquake coda. Bulletin. Seismological Society America, 90, 2, pp 512-524.

Frankel, A. and L. Wennerberg (1987). Energy-flux model of seismic coda: separation of scattering and intrinsic attenuation, *Bull. Seism. Soc. Am.* **77**, 1223-1251.

Furumoto, M., T. Kunitomo, H. Inoue, I. Yamada, K. Yamaoka, A. Ikami, and Y. Fukao (1990). Twin source of high-frequency volcanic tremor of Izu-Oshima Volcano, Japan. *Geophysical. Research Letters*, **17**, 25-27.

Humphreys, E., R. W. Clayton, and B. H. Hager (1984). A tomographic image of mantle structure beneath southern California. *Geophysical Research Letters*, **11**, 625-627.

Kak, A. C. and M. Slaney (1988). *Principles of computerized tomographic imaging*. IEEE Press, New York.

Nakanishi, I. (1985). Three-dimensional structure beneath the Hokkaido-Tohoku region as derived from a tomographic inversion of P-arrival times. *Journal Physics of the Earth*, 33, 241-256.
Nishigami, K. (1997). Spatial distribution of coda scatterers in the crust around two active volcanoes and one active fault system in central Japan: inversion analysis of coda envelope. *Physics of the Earth and Planetary Interiors*, 104, 75-89.
Ogilvie, J. S. (1988). Modeling of seismic coda, with application to attenuation and scattering in southeastern Tennessee, *M.S. Thesis*, Georgia Institute of Technology, Atlanta, Georgia.
Sato, H. (1977). Energy propagation including scattering effects: single isotropic sattering approximation. *J. Phys. Earth*, 25, 27-41.
Sun, Yonghe, F.Qin, S. Checkles, and J. P. Leveille, (2000). A beam approach to Kirchhoff depth imaging, *The Leading Edge.* 19, 1168-1173.
Revenaugh, J., (2000). The relation of crustal scattering to seismicity in southern California, *Journal of Geophysical Resarch,* 105, 25,403-25,422.